

Possible reaction pathways of selected organophosphorus and carbamate pesticides according to the DFT calculation method

B. Eren^{1*}, Y. Y. Gurkan²

¹Tekirdag Namik Kemal University, Faculty of Agriculture, Tekirdag, Turkey

²Tekirdag Namik Kemal University, Department of Chemistry, Tekirdag, Turkey

Accepted: July 14, 2022

This research was carried out in order to analyse the reactions of three organophosphorus (OP) and three carbamate (CB) pesticides with the hydroxyl radical (.OH), and their degradation paths. The studied organophosphorus pesticides are Azamethiphos, Coumaphos, Temephos, and the carbamate pesticides are Methiocarb, Carbofuran, Pirimicarb. Initially, in the reactions, the initial geometries of the reactants were determined. Geometric optimisations were performed using the DFT/B3LYP/6-31G (d) basic set of Quantum Mechanical Density Functional Theory (DFT). For each molecule, degradation reaction mechanisms were tried to be clarified using the calculated energy values. Since the reactions of pesticides with .OH are essential in terms of both water treatment and atmospheric chemistry, energy values were calculated both at gaseous phase and aqueous phase by modelling the solvent effect. For each molecule, fragments were found out by analysing the bond lengths, bond angles, and energy values, and as a result, degradation paths were determined.

Keywords: Organophosphorus pesticides, Carbamate pesticides, DFT

INTRODUCTION

Organophosphorus compounds have become the most widely used insecticides after the use of chlorinated hydrocarbons were restricted and banned due to the problems they caused. As a chemical structure, organophosphorus insecticides (OPs) are the esters of phosphoric acid (H₃PO₄). Methoxy (OCH₃) or ethoxy (OC₂H₅) are usually bound to the phosphorus atom as two ester groups. The third ester group may be aliphatic, homocyclic, or heterocyclic, and can be bound to the phosphorus atom *via* ester (P-O-R) or thioester (P-S-R) bonds. This weak bond increases the electrophilic property of the phosphorus atom, and brings in the electron withdrawing property. Physicochemical properties of active agents in different subgroups such as evaporation, water solubility, penetration into plant tissues, and their movement within plant tissues vary considerably. It is stated that this change mainly results from P = O or P = S structure, and also from organic structures from the third ester group. The persistence of OPs in nature is short due to their rapid degradation. These pesticides degrade quickly, thus do not lead to long-term damage; however, besides they kill the non-target insects they also harm both people and nature. In addition, since they do not have a stable structure, they are used frequently. Therefore, they are considered costly [1-9].

Carbamate pesticides (CBs) are able to transform into various products through oxidation, biotransformation, hydrolysis, biological growth,

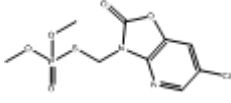
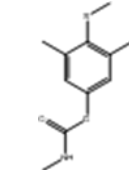
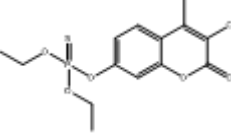
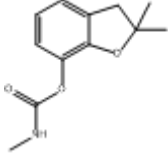
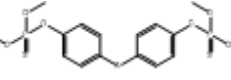
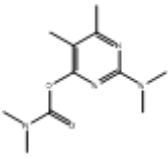
photolysis, biological degradation, as well as through metabolic reactions in living organisms [10]. Besides the ability to metabolise CBs, microbial populations can also make themselves congruent with many of the metabolites of CBs. These pesticides and their metabolites may affect the microflora and also the soil fertility. Although CBs are very stable at aqueous environments, the administration of these toxic compounds may lead to a considerable decrease in non-target organisms [11]. The main problem in the use of CBs is that they remain in the environment for a long time. Due to their high water solubility, their residues are able to circulate in aqueous environments by percolation from soil to soil or to surface waters. Moreover, their wide application in agriculture increases their residues in environmental matrices [12].

The two-dimensional figures, molecule names, abbreviations that will be used hereafter and molecule formulas of the six molecules analyzed in this research are given in Table 1. The pesticides were analyzed initially in terms of their structures: It is possible to analyse the OPs, which are organophosphorus, according to how sulfur, oxygen, nitrogen, and carbon atoms are bound. While methoxy was bound as two ester groups to P atom in OP1 and OP3 molecules, ethoxy was bound as two ester groups to P atom in OP2 molecule. There is P=O bond in OP1 while there is P=S instead of P=O in OP2 and OP3 molecules.

* To whom all correspondence should be sent:

E-mail: beren@nku.edu.tr

Table 1. Two-dimensional figures, molecule names, abbreviations and molecule formulas of the studied molecules.

Two-dimensional figure	Molecule name and formula	Two-dimensional figure	Molecule name and formula
	(OP1) Azamethiphos C ₉ H ₁₀ ClN ₂ O ₅ PS		(CB1) Methiocarb C ₁₁ H ₁₅ NO ₂ S
	(OP2) Coumaphos C ₁₄ H ₁₆ ClO ₃ PS		(CB2) Carbofuran C ₁₂ H ₁₅ NO ₃
	(OP3) Temephos C ₁₆ H ₂₀ O ₆ P ₂ S ₃		(CB3) Pirimicarb C ₁₁ H ₁₈ N ₄ O ₂

Since there are three O atoms and one S atom in all three molecules, all three OPs are called thiophosphates. Out of these three OPs, OP3 has a symmetric structure.

CBs, which are called carbamate compounds, and are carbamic acid esters, constitute a smaller group compared to the OPs. They are composed of a carboxyl (COO) instead of a hydrogen atom bound to an amine (NH₂) resulting in H₂N-COO-R structure. While there is one methyl group bound to N in CB1 and CB2 molecules, it is remarkable that there are two methyl groups bound to N in CB3 molecule. In all three molecules the R groups are different within H₂N-COO-R molecule structure.

All of the studied molecules are organic compounds, and it is known that organic pollutants are found in waters at low concentration levels. Biomolecules, which are hydroxyl radical scavengers and are various in terms of velocity, are specific detectors for hydroxyl radicals due to their hydroxylation capabilities. An attack of a hydroxyl radical to an aromatic compound leads to formation of a hydroxylated product, thus may be more dangerous than the original product at the beginning of the process. Therefore, it is essential that these products be observed [13].

METHODOLOGY

Theoretically, in order to determine all possible reaction paths of pesticides, geometric optimisations were performed using the DFT/B3LYP/6-31G (d) basic set of Quantum Mechanical Density Functional Theory (DFT). In all molecular orbital

calculations, energy values were calculated, and geometric optimisations were made by using Gauss View 5.0.8 molecular display programme and Gaussian 09 programme. Gauss View5.0.8 visualizes the molecules for the use of the Gaussian packaged software, and enables the rotation, movement, or any change of the molecules. It also permits the researcher to analyse all the calculated results of the Gaussian programme graphically [14]. The energy of the decomposition reaction of all organic compounds is affected by the water molecules in aqueous medium. In addition, the geometry stretch in the solutions is induced by H₂O. In other words, the presence of dielectric environment such as H₂O leads to geometric relaxation, and this results in an energy decreasing, and stabilising effect for the mechanism [13]. Therefore, in order to explain the solvent impact of H₂O on pesticide + ·OH reaction in this study, COSMO (conductor-like screening solvation model) within the Gaussian 09 packaged software was used [14]. Since the fate in the nature of the analysed three organophosphorus and three carbamate pesticides is important in terms of both atmospheric chemistry and water chemistry, the energy values in Table 2 and Table 3 are given in both aqueous and gaseous phases. Since the data obtained in atomic mass units when converted to kcal/mol unit started to differ from each other on the seventh digit, the results were given completely without rounding up the numbers. The bond lengths and bond angles given in the tables, which are apparently bigger, are highlighted as bold characters.

THEORETICAL RESULTS

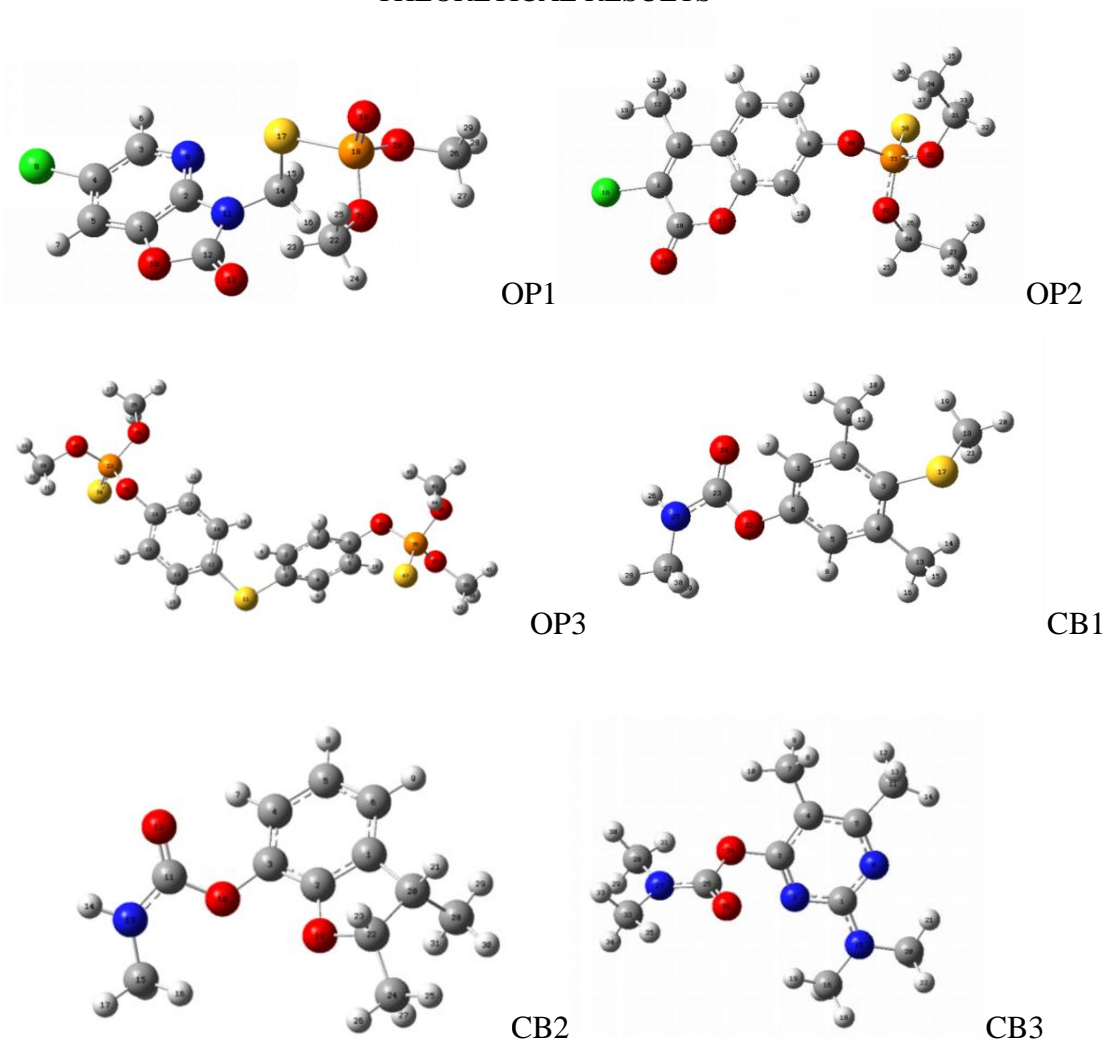


Figure 1. Optimized geometric structures of the studied molecules with DFT method (grey, C; white, H; blue, N; red, O; green, Cl; yellow, S; orange, P).

Table 2. Energy values of the gaseous and aqueous phases of OPs, and bond lengths and bond angles of atoms within OPs.

	Gaseous phase (kcal/mol)	Aqueous phase (kcal/mol)	Bond length	(Å)	Bond angle	(°)
OP1	-1,276,474.519	-1,276,484.148	O ₂₁ -C ₂₂	1.44823	C ₂₆ O ₂₀ P ₁₈	118.59736
	-1,276,473.927	-1,276,483.556	O ₂₀ -P ₁₈	1.61186	O ₂₀ P ₁₈ O ₂₁	99.44751
	-1,276,518.746	-1,276,529.022	O ₂₁ -P ₁₈	1.61665	P ₁₈ O ₂₁ C ₂₂	119.67896
			S ₁₇ -P ₁₈	2.10137	S ₁₇ P ₁₈ O ₂₁	107.77915
			S ₁₇ -C ₁₄	1.86825	C ₁₄ S ₁₇ P ₁₈	100.93849
			N ₁₁ -C ₁₄	1.43993	N ₁₁ C ₁₄ S ₁₇	111.14930
			O ₂₀ -C ₂₆	1.44569		
	OP2	-1,329,539.807	-1,329,549.935	Cl₁₆-C₁	1.74557	O ₂₂ C ₂₄ C ₂₇
-1,329,539.214		-1,329,549.343	C ₁₂ -C ₂	1.50422	O ₂₃ C ₃₁ C ₃₄	111.64910
-1,329,589.227		-1,329,599.736	O ₂₀ -C ₈	1.38960	O ₂₂ P ₂₁ S ₃₈	117.86055
			O₂₀-P₂₁	1.63745	O ₂₃ P ₂₁ S ₃₈	117.57544
			S₃₈-P₂₁	1.93952	O ₂₀ P ₂₁ O ₂₂	99.98248
			O₂₃-P₂₁	1.60469	O ₂₀ P ₂₁ O ₂₃	99.81860

			O22-P21 O22-C24 C24-C27 O23-C31 C31-C34	1.60503 1.45472 1.51907 1.45341 1.51927	C ₈ O ₂₀ P ₂₁ O ₂₀ P ₂₁ S ₃₈	122.55848 116.43632
OP3	-1,851,213.200 -1,851,212.608 -1,851,276.348	-1,851,225.391 -1,851,224.798 -1,851,288.619	O ₃₇ -C ₃₉ O ₃₈ -C ₄₃ O ₃₈ -P ₃₆ O ₃₇ -P ₃₆ S47-P36 O ₃₅ -P ₃₆ O ₆ -O ₃₅ S ₁₁ -C ₃ S ₁₁ -C ₁₂ O ₂₅ -C ₃₀ O ₂₄ -C ₂₅ O ₂₄ -P ₂₃ O ₂₅ -P ₂₃ S34-P23 O ₂₂ -P ₂₃ O ₂₂ -C ₁₉	1.44123 1.43965 1.61018 1.60977 1.93700 1.62704 1.39693 1.79378 1.79393 1.43951 1.44147 1.61068 1.61038 1.93616 1.62655 1.39522	C ₄₃ O ₃₈ P ₃₆ C ₃₉ O ₃₇ P ₃₆ C ₆ O ₃₅ P ₃₆ O ₃₅ P ₃₆ S ₄₇ S ₄₇ P ₃₆ O ₃₈ C ₃₀ O ₂₅ P ₂₃ C ₂₆ O ₂₄ P ₂₃ O ₂₄ P ₂₃ O ₂₂ S ₃₄ P ₂₃ O ₂₂ P ₂₃ O ₂₂ C ₁₉ C ₁₂ S ₁₁ C ₃	120.76411 120.56106 123.21190 117.32956 117.40393 120.79832 120.28954 100.46100 117.52168 124.60188 103.30950

Table 3. Energy values of the gaseous and aqueous phases of CBs, and bond lengths and bond angles of atoms within CBs.

	Gaseous phase (kcal/mol)	Aqueous phase (kcal/mol)	Bond length	(Å)	Bond angle	(°)
CB1	-647,184.4656 -647,183.8726 647,224.4561	-647,190.0072 -647,189.4148 -647,230.3271	N ₂₅ -C ₂₇ N ₂₅ -C ₂₃ O ₂₂ -C ₂₃ O ₂₂ -C ₆ S17-C18 S17-C3 C ₄ -C ₁₃	1.45499 1.36217 1.37696 1.39141 1.83693 1.80236 1.51156	C27N25C23 N ₂₅ C ₂₃ O ₂₂ C ₂₃ O ₂₂ C ₆ C ₁₈ S ₁₇ C ₃ S ₁₇ C ₃ C ₄ C3C4C13 C ₅ C ₄ C ₁₃	126.20337 109.57643 120.62380 101.01669 119.64032 122.31470 118.94762
CB2	-468,420.1723 -468,419.5800 -468,457.6359	-468,428.6023 -468,428.0093 -468,466.1173	N13-C15 N ₁₃ -C ₁₁ O ₁₀ -C ₁₁ O ₁₀ -C ₃ C22-C24 C20-C28 O19-C22	1.45464 1.36116 1.37639 1.38867 1.51697 1.53876 1.46116	C15N13C11 N ₁₃ C ₁₁ O ₁₀ C ₁₁ O ₁₀ C ₃ C ₁ C ₂₀ C ₂₈ O ₁₉ C ₂₂ C ₂₄ C ₂₀ C ₂₂ C ₂₄ C ₂₂ C ₂₀ C ₂₈	126.26617 109.50848 119.94145 111.71001 108.41780 118.30637 115.53466
CB3	-501,498.9604 -501,498.3680 -501,543.1276	-501,505.8385 -501,505.2455 -501,549.6004	N27-C28 N27-C32 N ₂₇ -C ₂₅ O ₂₆ -C ₂₅ O ₂₄ -C ₂₅ O ₂₄ -C ₃ N15-C20 N15-C16 N ₁₅ -C ₁ C5-C11 C4-C7	1.45428 1.45430 1.36415 1.21252 1.38970 1.38378 1.45156 1.45190 1.37002 1.50775 1.50604	C ₂₀ N ₁₅ C ₁ C ₁ N ₁₅ C ₁₆ C ₂₀ N ₁₅ C ₁₆ C ₂₅ N ₂₇ C ₂₈ C ₃₂ N ₂₇ C ₂₈ C ₃₂ N ₂₇ C ₂₈ N ₂₇ C ₂₅ O ₂₄ O24C25O26 N27C25O26 C ₂₅ O ₂₄ C ₃	121.76976 121.43061 116.28654 124.91824 116.57136 116.57136 110.73159 123.22908 125.97465 117. 6189

Table 4. Energy values of fragments of OP molecules in gaseous phase.

OP	Gaseous phase (kcal/mol)	OP	Gaseous phase (kcal/mol)	OP	Gaseous phase (kcal/mol)
OP1	$\Delta E = -1,276,474.519$ $\Delta H = -1,276,473.927$ $\Delta G = -1,276,518.746$	OP2	$\Delta E = -1,329,539.807$ $\Delta H = -1,329,539.214$ $\Delta G = -1,329,589.227$	OP3	$\Delta E = -1,851,213.200$ $\Delta H = -1,851,212.608$ $\Delta G = -1,851,276.348$
OP1 ₁	-1,251,829.351 -1,251,828.758 -1,251,828.758	OP2 ₁	-1,304,885.400 -1,304,884.808 -1,304,933.008	OP3 ₁	-1,826,567.746 -1,826,567.153 -1,826,627.826
OP1 ₂	-1,252,288.284 -1,252,287.691 -1,252,325.969	OP2 ₂	-1,280,118.360 -1,280,230.069 -1,280,276.369	OP3 ₂	-1,801,922.162 -1,801,921.570 -1,801,980.884
OP1 ₃	-963,425.967 -963,425.374 -963,464.772	OP2 ₃	-1,280,239.707 -1,280,239.115 -1,280,284.604	OP3 ₃	-1,801,922.622 -1,801,922.029 -1,801,980.023
OP1 ₄	-988,081.157 -988,080.564 -988,123.768	OP2 ₄	-1,280,231.280 -1,280,230.688 -1,280,276.632	OP3 ₄	-1,050,909.013 -1,050,908.421 -1,050,948.843
OP1 ₅	-596,452.829 -596,452.236 -596,478.917	OP2 ₅	-1,041,138.508 -1,041,137.915 -1,041,185.763	OP3 ₅	-1,752,631.045 -1,752,630.453 -1,752,684.711
OP1 ₆	-308,049.323 -308,048.730 -308,073.243	OP2 ₆	-1,304,885.648 -1,304,885.056 -1,304,933.369	OP3 ₆	-1,243,036.585 -1,243,035.993 -1,243,084.858
OP1 ₇	-621,105.140 -621,104.548 -621,134.006	OP2 ₇	-1,016,484.104 -1,016,483.511 -1,016,529.431	OP3 ₇	-634,859.235 -634,858.642 -634,894.182
OP1 ₈	-870,967.493 -870,966.900 -870,998.630	OP2 ₈	-1,016,483.333 -1,016,482.740 -1,016,529.052	OP3 ₈	-1,777,276.851 -1,777,276.258 -1,777,332.407
OP1 ₉	-1,132,742.293 -1,132,741.700 -1,132,777.662	OP2 ₉	-1,255,576.546 -1,255,575.954 -1,255,620.102	OP3 ₂₁	-1,754,705.068 -1,754,704.476 -1,754,761.596
OP1 ₁₀	-963,441.125 -963,440.532 -963,477.748	OP2 ₁₀	-1,230,930.996 -1,230,930.404 -1,230,971.800	OP3 ₂₂	-1,707,485.222 -1,707,484.629 -1,707,539.171
OP1 ₁₁	-1,204,609.012 -1,204,608.420 -1,204,648.722	OP2 ₁₁	-1,206,285.055 -1,206,284.463 -1,206,323.472	OP3 ₂₃	-1,195,840.766 -1,195,840.173 -1,195,888.033
OP1 ₁₂	-938,785.100 -938,784.508 -938,820.472	OP2 ₁₂	-672,054.408 -672,053.815 -672,085.640	OP3 ₉	-540,468.308 -540,467.716 -540,499.397
OP1 ₁₃	-891,565.651 -891,565.058 -891,599.512	OP2 ₁₃	-624,858.313 -624,857.721 -624,887.961	OP3 ₅₁	1,705,413.934 -1,705,413.342 -1,705,465.073
OP1 ₁₄	-844,339.253 -844,338.661 -844,372.455			OP3 ₅₂	-1,658,196.793 -1,658,196.200 -1,658,246.328

Table 5. Energy values of fragments of CB molecules at gaseous phase.

CB	Gaseous phase (kcal/mol)	CB	Gaseous phase (kcal/mol)	CB	Gaseous phase (kcal/mol)
CB1	$\Delta E = -646,961.779$ $\Delta H = -647,183.873$ $\Delta G = -647,224.456$	CB2	$\Delta E = -468,420.172$ $\Delta H = -468,419.580$ $\Delta G = -468,457.636$	CB3	$\Delta E = -501,498.960$ $\Delta H = -501,498.368$ $\Delta G = -501,543.128$
CB1 ₁	-622,534.677 -622,534.084 -622,571.718	CB2 ₁	-443,769.090 -443,768.498 -443,803.804	CB3 ₁	-476,849.737 -476,849.145 -476,891.558
CB1 ₂	-622,531.874 -622,531.282 -622,569.784	CB2 ₂	-443,766.239 -443,765.647 -443,802.036	CB3 ₂	-476,851.211 -476,850.618 -476,892.847
CB1 ₃	-622,532.928 -622,532.335 -622,570.695	CB2 ₃	-419,114.956 -419,114.363 -419,147.993	CB3 ₃	-476,846.201 -476,845.608 -476,888.095
CB1 ₄	-597,881.471 -597,880.879 -597,916.436	CB2 ₄	-394,462.904 -394,462.312 -394,494.120	CB3 ₄	-476,836.756 -476,836.164 -476,877.675
CB1 ₅	-587,878.743 -597,878.151 -597,914.624	CB2 ₅	-288,617.636 -288,617.670 -288,642.136	CB3 ₇	-476,851.211 -476,850.618 -476,892.842
CB1 ₆	-597,883.246 -597,882.653 -597,917.775	CB2 ₆	-241,425.820 -241,425.227 -241,448.596	CB3 ₈	-452,202.855 -452,202.263 -452,241.368
CB1 ₇	-573,227.718 -573,227.125 -573,261.071			CB3 ₆	-452,189.581 -452,188.988 -452,228.523
CB1 ₈	-323,363.666 -323,363.074 -323,393.491			CB3 ₉	-417,469.381 -417,468.789 -417,506,179
CB1 ₉	-298,712.157 -298,711.564 -298,739.598			CB3 ₁₀	-392,820.116 -392,819.523 -392,855.204
CB1 ₁₀	-442,728.940 -442,728.348 -442,752.493			CB3 ₁₁	-368,174.342 -368,173.750 -368,206.206
CB1 ₁₁	-395,536.578 -395,535.985 -395,558.810			CB ₃₅	-346,360.378 -346,359.785 -346,393.973
CB1 ₁₂	-192,864.522 -192,863.930 -192,885.827			CB3 ₁₂	-262,331.250 -262,330.658 -262,357.466
CB1 ₁₃	-145,672.144 -145,671.552 -145,692.129			CB3 ₁₃	-165,814.401 -165,813.808 -165,834.192

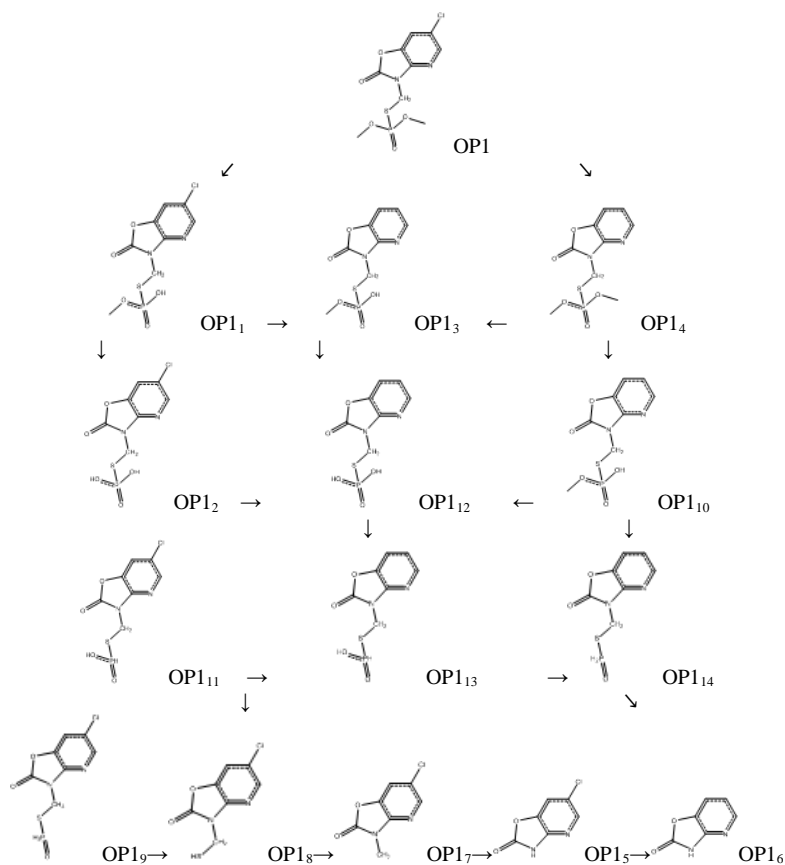


Figure 2. Degradation mechanism of OP1 molecule.

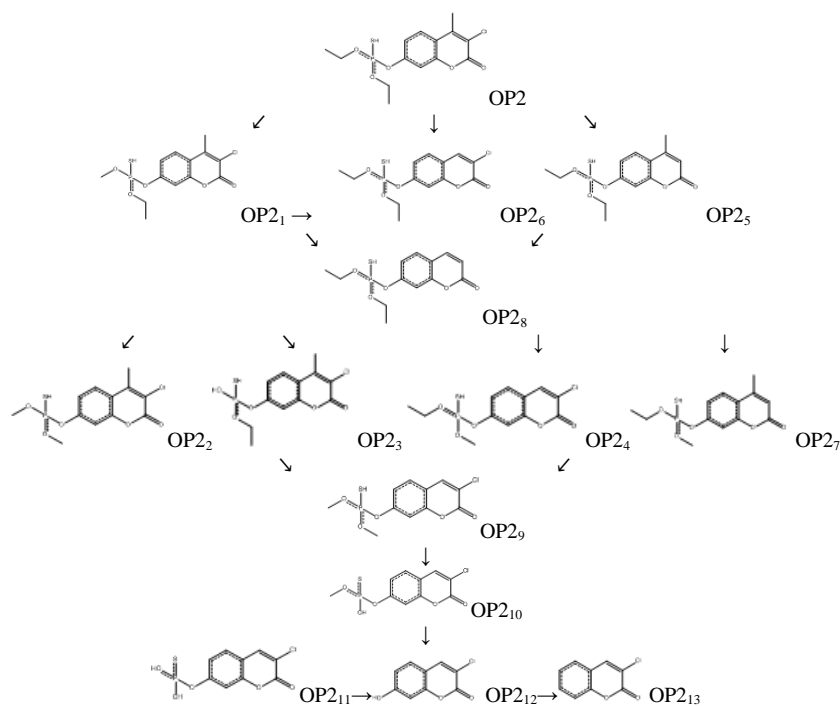


Figure 3. Degradation mechanism of OP2 molecule.

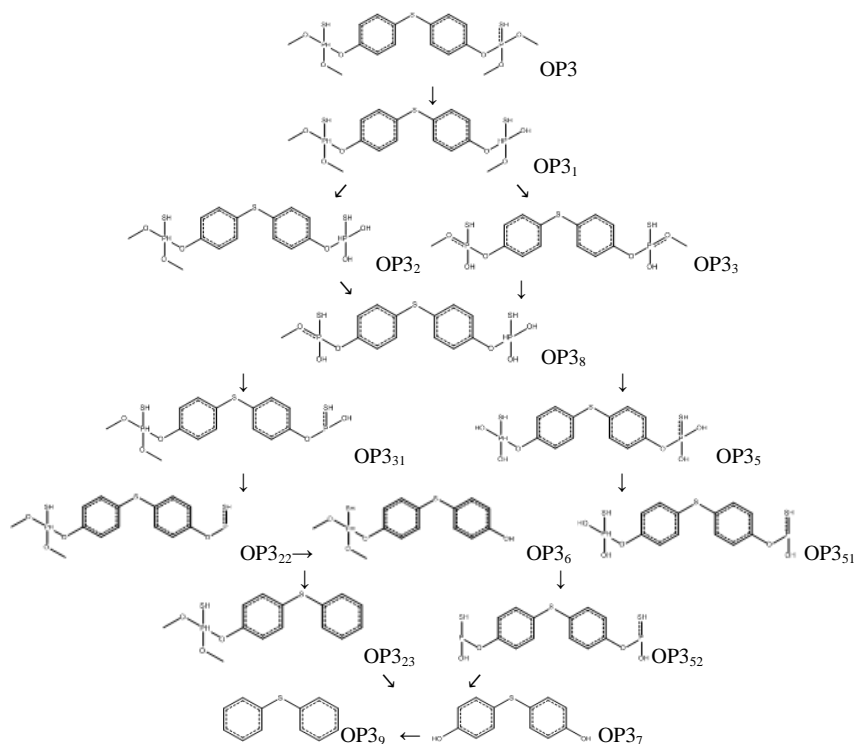


Figure 4. Degradation mechanism of OP3 molecule.

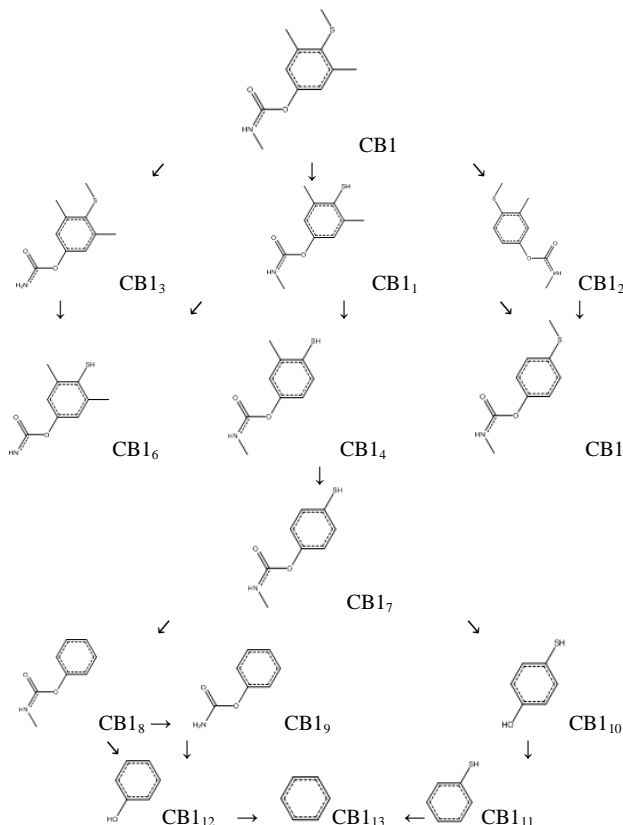


Figure 5. Degradation mechanism of CB1 molecule.

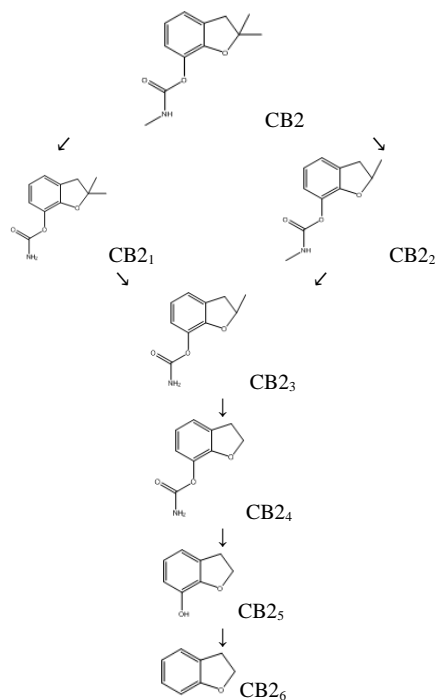


Figure 6. Degradation mechanism of CB2 molecule.

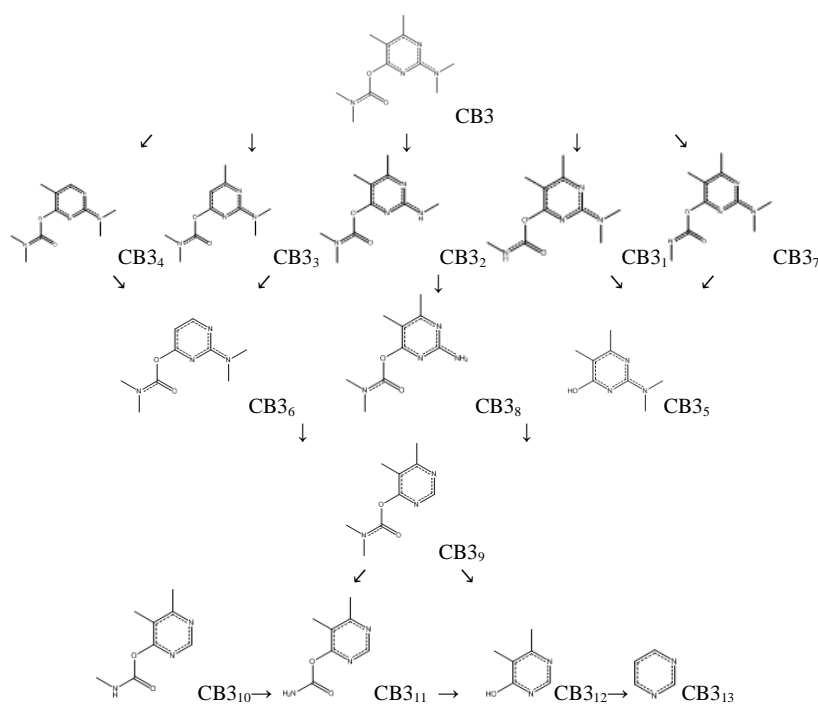


Figure 7. Degradation mechanism of CB3 molecule

CONCLUSION

While the degradation mechanism was obtained for each molecule, bond lengths and bond angles of all atoms within all molecules and energy values of each fragment were analyzed individually, it was tried to make estimations starting from the one with the lowest energy, in other words, the most spontaneous fragment; also considering the ones with the longest bond length, and the one with the widest bond angle, or the most stable structures

bound with double bonds. In order to exemplify what has been considered during these estimations, below there are explanations for one sample for each pesticide group, namely OP1 and CB1.

O₁₉ and O₁₃ in OP1, as also seen in Figure 1, form double bonds with P₁₈ and C₁₂ atoms, respectively. Since these bonds are stable, they are not expected to break. Bond lengths of O₂₁-C₂₂ and O₂₀-C₂₆ in Table 2 are 1.44823 Å; 1.44569 Å, respectively. Again in the same Table, the first and second wide

bond angles are the ones of $P_{18}O_{21}C_{22}$ with the bond angle 119.67896° , and the ones of $P_{18}O_{20}C_{26}$ with the bond angle 118.59736° . In the light of this information, the methyl groups including C_{26} and C_{22} atoms are expected to break. Whether the methyl groups were the first of the fragmentation paths was determined by analysing their energy values. The OP_{11} and OP_{12} fragments in Figure 2 confirm this prediction. N_{11} is an electronegative atom. When the space surrounded by this atom was observed, it was found that $N_{11}-C_{14}$ in Table 2 has a bond length of 1.43993 \AA , and since there are longer bond lengths than this one, it was predicted that if there were to be any bond break there, it would be subsequent to the break of the other bonds. In Figure 2, the degradation of the N-bond in the final stages of the cleavage pathway proves this thesis. The bond lengths of $S_{17}-P_{18}$ and $S_{17}-C_{14}$ in Table 2 are the longest bonds in the molecule with 2.10137 \AA ; 1.86825 \AA respectively. When the bond formed by S breaks, phosphate will leave the molecule. In Table 4, energy values of the fragments at gaseous phase were analysed. The degradation path for OP1 in Figure 2 was determined starting from the fragment with the lowest energy level, in other words, from the most spontaneous fragment, considering both the above given predictions and the energy values for each fragment given in Table 4.

O_{22} in CB1 molecule given in Figure 1 is an electronegative atom. When the space surrounded by this atom was observed, it was found out that the $C_{23}O_{22}C_6$ bond angle was 120.62380° , $O_{22}-C_{23}$ bond length was 1.37696 \AA , and $O_{22}-C_6$ bond length was 1.39141 \AA as given in Table 3. Since in terms of bond angles there are wider angles than this, and since there are bond lengths longer than the above given one, if there were to be a bond break there, it would occur subsequent to the other bond breaks. The break from O_{22} in the molecule is in the final stage of degradation, as can be seen in Figure 5. As seen in Figure 1, since O_{24} is bound to C_{23} with a double bond, it is stable, and this bond is not expected to break. Although N_{25} is an electronegative atom, in Table 3, $C_{27}N_{25}C_{23}$ in its optimized form is the widest bond angle of the molecule with 126.20337° . The bond length $N_{25}-C_{27}$ is the longest with 1.45499 \AA in the same table. We can understand from here that the methyl group C_{27} attached to N_{25} will break off in the first place. This bond length comes after the bond lengths made by S_{17} and C_4 atoms. The width of the bond angle competes with these bond lengths. For S_{17} atom, $S_{17}-C_{18}$ bond in Table 3 is ready to break with the longest bond length in the molecule as 1.83693 \AA . $C_3C_4C_{13}$ bond angle in the same table with 122.31470° is a

preview of a methyl group being ready to detach from the molecule. Methyl groups including C_9 , C_{13} , C_{18} , C_{27} atoms are remarkable in terms of their first fragmentation paths. Predicting that the break will start here, energy values at gaseous phase of the fragments in Table 5 were analysed. First, methyl groups were detached one by one, and CB_{11} , CB_{12} , CB_{13} were obtained, then binary breakings were analysed, and CB_{14} , CB_{15} , CB_{16} fragments gained their place in the decomposition reaction. Starting with the fragment with the lowest energy level, in other words with the most spontaneous one, degradation path of CB1 was determined by both the above given predictions and by the analysis of the energy values given in Table 5 for each fragment.

DISCUSSION

Degradation mechanism for the six molecules, which were studied in this research were predicted, and are given in Figures 3-7, respectively. Due to having the lowest energy values, OP3 among organophosphorus pesticides, and CB1 among carbamate pesticides were determined to be the most spontaneous molecules to react. It is predicted that the reason of OP3 to react as the most spontaneous molecule among other molecules of its group is its having a symmetric structure. However, the reason of CB1 molecule to react as the most spontaneous molecule among its group is the R group within $H_2N-COO-R$ molecular structure.

This study is compiled of the data obtained in the PhD dissertation, in which seven pesticides in total were analysed both theoretically and experimentally. Experimental and theoretical results for Phosmet, one of these seven pesticides, have been published [1]. The degradation reactions under the influence of light of the selected seven pollutants in aqueous TiO_2 suspensions were analysed experimentally as well. It was also established that when light and TiO_2 were in the same environment together, all the matters degraded to a large extent. The concentration changes at the end of 100 minutes were calculated as 78% for OP1, 85% for OP2, 76% for OP3, 87% for CB1, 95% for CB2, 94% for CB3. These results show that OP2 among organophosphorus pesticides, and CB2 among carbamate pesticides are the pesticides with the greatest degradation. According to the k rate constant, OP3 among organophosphorus pesticides, and CB1 among carbamate pesticides are the most rapid ones, since these two molecules have a greater constant rate among their own groups with 9.55 ± 0.006 10.35 ± 0.002 , respectively, and thus react faster than the others. The experimental results also indicate that OP1 and CB3 molecules are the

most spontaneous ones during reaction among their own groups.

Acknowledgements: The authors greatly appreciate Namik Kemal University Research Foundation for financial support. Project number: NKUBAP.01.GA.20.260 The authors declare that there is no conflict of interests regarding the publication of this paper.

REFERENCES

1. B. Eren, Y. Yalçın Gürkan, *Bulgarian Chemical Communications*, **53** (4), 456 (2021).
2. R. Atkinson, S. M. Aschmann, M. A. Goodman, A. M. Winer, *Int. J. Chem. Kinet.*, **20**, 273 (1988).
3. M. A. Goodman, S. M. Aschmann, R. Atkinson, A. M. Winer, *Arch. Environ. Contam. Toxicol.*, **17**, 281 (1988).
4. M. A. Goodman, S. M. Aschmann, R. Atkinson, A. M. Winer, *Environ. Sci. Technol.*, **22**, 578 (1988).
5. R. Atkinson, J. Arey, *Chem. Rev.*, **103**, 4605 (2003).
6. S. M. Aschmann, E. C. Tuazon, R. Atkinson, *J. Phys. Chem. A*, **109**, 11828 (2005).
7. S. M. Aschmann, E. C. Tuazon, R. Atkinson, *J. Phys. Chem. A*, **109**, 2282 (2005).
8. S. M. Aschmann, R. Atkinson, *J. Phys. Chem. A*, **110**, 13029 (2006).
9. S. M. Aschmann, E. C. Tuazon, W. D. Long, R. Atkinson, *J. Phys. Chem. A*, **114**, 3523 (2010).
10. Z. Q. Cai, J. Wang, J. T. Ma, X. L. Zhu, J. Y. Cai, G. H. Yang, *Journal of Agricultural and Food Chem.*, **63**, 7151 (2015).
11. M. Gupta, S. Mathur, T.K. Sharma, M. Rana, A. Gairola, N. K. Navani, R. Pathania, *Journal of Hazardous Materials*, **301**, 250 (2016).
12. M. Sturini, E. Fasani, C. Prandi, A. Casaschi, A. Albini, *J. Photochem, Photobiol. A: Chem.*, **101**, 251 (1996).
13. B. Eren, Y. Yalçın Gürkan, *JSCS*, **82** (3), 277 (2017).
14. Gaussian 09, Revision B.04, Gaussian Inc., Pittsburgh, PA, (2009).